Mineralogical Magazine, December 2003, Vol. 67(6), pp. 1193–1204

Microscopic and spectroscopic investigation of the calcite surface interacted with Hg(II) in aqueous solutions

A. GODELITSAS[1,*], J. M. ASTILLEROS[1,2], K. R. HALLAM[3], J. LÖNS[1] AND A. PUTNIS[1]

[1] Institut für Mineralogie, Universität Münster, Corrensstraße 24, D-48149 Münster, Germany
[2] Departamento de Cristalografía y Mineralogía, Universidad Complutense de Madrid, 28040 Madrid, Spain
[3] Interface Analysis Centre, University of Bristol, 121 St. Michael's Hill, Bristol BS2 8BS, UK

ABSTRACT

The interaction of the $\{10\bar{1}4\}$ cleavage surface of calcite with $Hg(CH_3COO)_2$ aqueous solutions with concentration of 5 mM Hg(II) (pH $\approx$3.5), was investigated using microscopic and spectroscopic techniques. *In situ* atomic force microscopy experiments showed that surface microtopography changes significantly as a result of the interaction, and that the initial rhombic etch pits induced by H_2O dissolution are rapidly transformed to deeper etch pits exhibiting an unusual triangular shape. The growth of these etch pits is strongly anisotropic, moving faster along the $[2\bar{2}1]$ direction than along the [010] direction (with step-retreat velocities of ~12 nm s^{-1} and ~4 nm s^{-1}, respectively). The modified etch pits are due to Hg(II) sorption in the surface, rather than due to the effect of the acetate anion. The sorption (adsorption and probably absorption also) of Hg(II), in the first minutes of the interaction, is shown by X-ray photoelectron spectroscopy. After ~2 h, the triangular etch pits are interconnected to form larger hexagonal etch pits, while Hg(II)-bearing phases (confirmed later by SEM-EDS) grow onto the surface through a heterogeneous nucleation process. The crystal growth of orthorhombic (montroydite-type) hydrated Hg(II) oxide ($HgO{\cdot}nH_2O$) on the surface of calcite was confirmed by XRD patterns and FT-IR spectra from samples exposed for longer times to $Hg(CH_3COO)_2$ solution.

KEYWORDS: calcite, cleavage surfaces, dissolution, sorption, crystal growth, mercury.

Introduction

THE dissolution and precipitation behaviour of calcite in aqueous media containing dissolved heavy metals is a subject of current research in earth, chemical and environmental sciences. Calcite interacts strongly with several divalent metal ions (Me^{2+}), removing them from aqueous solutions by sorption processes such as surface precipitation/coprecipitation, adsorption, and absorption/solid-state diffusion (e.g. Stipp *et al.*, 1992; Hay *et al.*, 2003; Godelitsas *et al.*, 2003). The sorption processes occur simultaneously with the dissolution of the surface of calcite. Surface precipitation/coprecipitation is associated with heterogeneous nucleation/crystal growth processes, leading to the formation of metal carbonate ($MeCO_3$) and hydroxycarbonate phases which are overgrown or deposited on the surface of the crystals. The potential formation of solid solutions, i.e. $(Me,Ca)CO_3$, during growth processes is also an important issue when discussing sorption processes (e.g. Paquette and Reeder, 1995; Reeder, 1996; Tesoriero and Pankow, 1996; Rimstidt *et al.*, 1998; Temmam *et al.*, 2000; Putnis *et al.*, 2003) in natural and industrial systems.

The chemical processes occurring on calcite surfaces can be studied *in situ* in a fluid cell of an Atomic Force Microscope (AFM) by observing and recording the dynamic evolution of the surface microtopography at a submicron scale. Considerable work has already been carried out on the interaction of calcite with pure, acidic and alkaline aqueous solutions (e.g. Hillner *et al.*, 1992; Stipp *et al.*, 1994; Liang *et al.*, 1996; Liang and Baer, 1997; Lea *et al.*, 2001; De Giudici

* E-mail: athgod@nwz.uni-muenster.de
DOI: 10.1180/0026461036760158

2002) and in the presence of various organic molecules (e.g. Britt and Hlady, 1997; Hong *et al.*, 1997; Teng and Dove, 1997; Teng *et al.*, 1998; Orme *et al.*, 2001). Studies by AFM on the interaction of calcite surfaces with dissolved metal ions, include Na^{+}, Mg^{2+}, Mn^{2+}, Sr^{2+}, Cd^{2+}, Ba^{2+}, La^{3+}, Eu^{3+} and Pb^{2+} (Davis *et al.*, 2000; Astilleros *et al.*, 2000; Shiraki *et al.*, 2000; Lea *et al.*, 2001; Astilleros *et al.*, 2002; Kamiya *et al.*, 2002; Astilleros *et al.*, 2003; Stipp *et al.*, 2003; Lea *et al.*, 2003; Hay *et al.*, 2003; Godelitsas *et al.*, 2003). While *in situ* AFM mainly shows the topographic effects of dissolution and growth processes, quantitative information on the subsequent sorption processes can be obtained using surface spectroscopic techniques such as X-ray Photoelectron Spectroscopy (XPS) and Rutherford Backscattering Spectroscopy (RBS) in combination (e.g. Stipp *et al.*, 2003; Hay *et al.*, 2003; Godelitsas *et al.*, 2003).

The main objective of this study was to characterize, by means of microscopic (*in situ* AFM, SEM-EDS), spectroscopic (XPS, FT-IR) and XRD techniques, the $\{10\bar{1}4\}$ cleavage surface of calcite interacted with aqueous solutions of a Hg(II) salt, ($Hg(CH_3COO)_2$). As a consequence, the chemical processes taking place simultaneously or in sequence at the calcite-water interface, during the interaction, can be recognized and distinguished. Special attention was given to the elucidation of the surface processes occurring during the initial stages of the interaction (1 to 5 min). Data of a similar nature on the interaction between calcite single crystals and other divalent metal ions such as Ni^{2+} and Pb^{2+} have recently been published (Hoffman and Stipp, 2001; Godelitsas *et al.*, 2003).

Experimental methods

The mm-sized calcite single crystals used in the present study were prepared by cleaving a chemically pure larger crystal of optical quality calcite from Chihuahua (Mexico), supplied by Dr F. Krantz (Bonn/D). All experiments involving the exposure of freshly cleaved $\{10\bar{1}4\}$ calcite surfaces to the Hg(II) solutions were performed at room temperature under atmospheric P_{CO_2}. The metal aqueous solutions, at a concentration of 5 mM Hg(II), were prepared using $Hg(CH_3COO)_2$ (Alfa Aesar), in the absence of background electrolyte in order to avoid additional elements interacting with the surface. Such solutions are naturally acidic (pH $\approx$3.5), containing hydrated Hg^{2+} ions as the dominant cationic species and limited amounts of hydrolysis products (Baes and Mesmer, 1986). Relevant information on the speciation of Hg(II) in the $Hg(CH_3COO)_2$ solutions used in the experiments were obtained using the PHREEQC program and the MINTEQ database (Parkhurst and Appelo, 1999). The rhombohedral calcite crystals were not chemically pre-treated, and the newly cleaved surfaces were in contact with nothing but air before exposure to distilled water and/or to Hg(II) solutions.

In the first set of experiments, *in situ* AFM images (both deflection and height) were obtained using the fluid cell of a Digital Instruments Nanoscope III Multimode instrument working in contact mode. Suitable calcite crystals were first interacted with distilled H_2O (~1 min) and then the changes in the surface microtopography were recorded after injection of Hg(II) solution (for up to ~2 h). The crystals removed from the AFM fluid cell were further examined by SEM-EDS using a Jeol JSM-6300F system equipped with an Oxford Instruments Link EDS system. At the same time, *in situ* AFM experiments were also carried out, for comparative purposes, using only a 0.006 M CH_3COOH (Merck) aqueous solution of pH $\approx$3.5.

In the second set of experiments, in order to obtain samples for the spectroscopic (XPS) investigations, freshly-cleaved crystals were reacted, into 50 ml sterile polypropylene Tubes (Greiner Bio-One), for different periods of time (1, 5 and 20 min). The methodology indicated by Hoffmann and Stipp (2001) was generally followed. The crystals were immersed in Hg(II) solution, and held in constant motion for a given period of time, by holding two of their edges with Teflon tweezers. At the end of the exposure time, each crystal was removed and the remaining droplets were blown from the surface using a stream of high-purity N_2. Then, the Hg(II)-interacted calcite samples were introduced into the vacuum chamber for spectroscopic investigations, adjusted carefully in stainless-steel holders. The XPS spectra were obtained using a VG Escascope and Mg-$K\alpha$ X-rays (charge-correcting the spectra on the basis of the adventitious hydrocarbon C 1s signal at 284.8 eV).

Finally, in the third set of experiments, calcite single crystals were exposed for longer periods (from 12 h to 1 month) to Hg(II) solutions. The solid experimental products were characterized by means of powder X-ray diffraction (powder-XRD) using a Philips X'Pert diffractometer with Cu-$K\alpha$ radiation, whereas mid-FT-IR (infrared)

spectra were recorded using a Bruker Vector 22 spectrometer and KBr pellets. Natural montroydite (HgO) crystals, from Socrates mine CA/USA (supplied by Excalibur Mineral Corp., NY/USA) were also examined using the above techniques.

Results and discussion

Short term (1–5 min) interaction of calcite surface with Hg(II) solution

In situ AFM observations on a calcite cleavage surface interacted with H_2O (pH $\approx$7) for ~1 min and subsequently with a $Hg(CH_3COO)_2$ aqueous solution (pH $\approx$3.5), containing 5 mM Hg(II), up to 5 min, are shown in Fig. 1. The preliminary injection of distilled water into the AFM fluid cell is required to clean the calcite surface as well as to establish the crystallographic directions on the {10$\bar{1}$4} face from the orientation of the etch pits. These characteristic rhombic etch pits (Fig. 1*a*) are defined by dissolution steps aligned along [$\bar{4}$41] and [48$\bar{1}$] directions. The faces of these steps are not equivalent and they are designated "+" (obtuse) and "–" (acute); the $[\bar{4}41]_+$ and

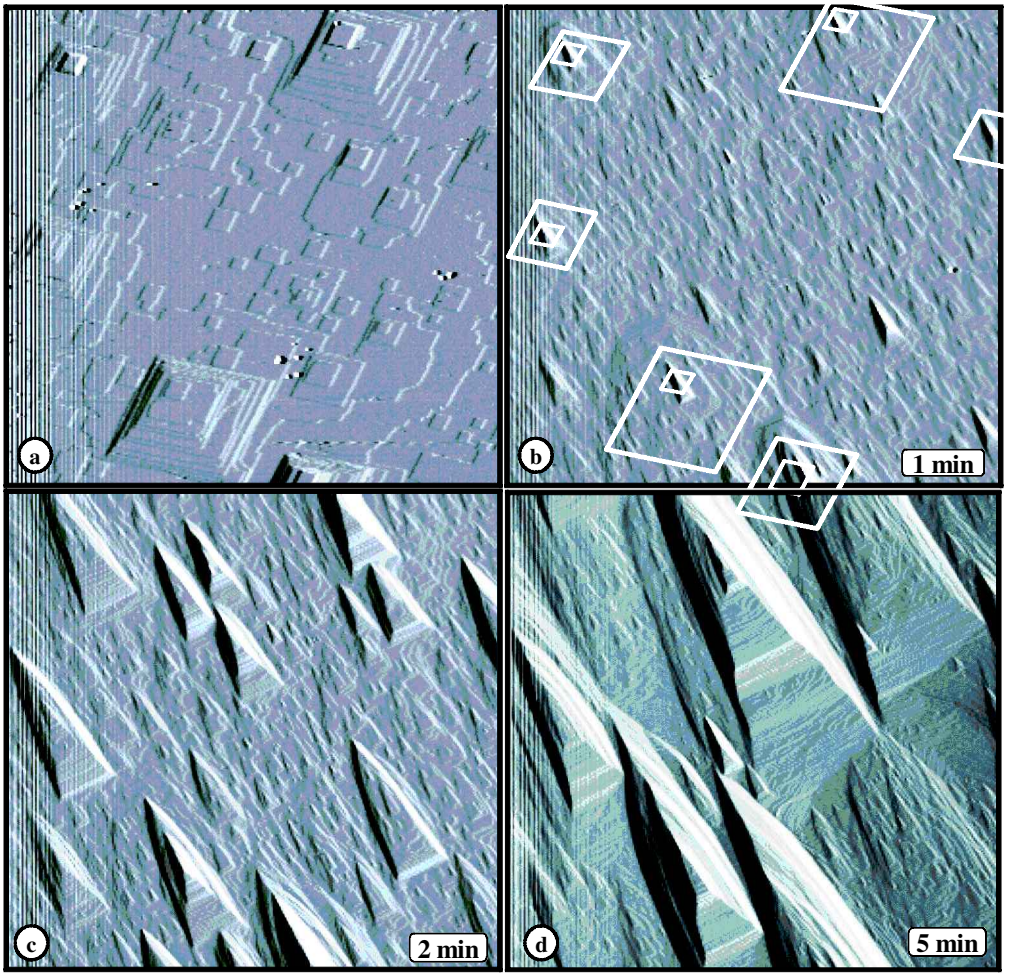

FIG. 1. A time sequence of *in situ* contact mode AFM images (deflection) showing the dynamic evolution of the freshly-cleaved {10$\bar{1}$4} calcite surface microtopography, during the interaction with distilled water (*a*), and further after injection of Hg(II) acetate aqueous solution of 5 mM Hg(II) and pH ~3.5 (*b*–*d*), at room temperature and atmospheric P_{CO_2}. The white outlines in *b* mark the location of the original H_2O-induced etch pits shown in *a*. The scan area is 7.5×7.5 μm^2. The vertical faintly-white lines at the left side of each image represent an artefact due to the fast scanning required in order to observe the changes in the surface microtopography.

$[48\bar{1}]_+$ steps are symmetrically related as are the $[\bar{4}41]_-$ and $[48\bar{1}]_-$ steps. This non-equivalence results in an anisotropic dissolution rate in water, with the obtuse steps advancing faster than the acute steps (e.g. Hillner *et al.*, 1992; Stipp *et al.*, 1994; Liang *et al.*, 1996; Liang and Baer, 1997; Lea *et al.*, 2001; De Giudici, 2002). At pH ≈9 (adjusted by NaOH) the step-retreat velocities are 3.4 nm s^{-1} and 1.5 nm s^{-1} respectively (Liang and Baer, 1997), whereas in the pH region 4.3–7.5 (adjusted by HCl), the respective velocities are 4.2 nm s^{-1} and 1.1 nm s^{-1} (De Giudici, 2002).

In our experiments, the initial H_2O-induced rhombic etch pits disappear rapidly after injection of the $Hg(CH_3COO)_2$ solution, and are replaced by deeper etch pits in the shape of an isosceles triangle with slightly curved sides (Fig. 1*b–d*). The transformation of the etch pits is exceptionally rapid, and as a result the entire surface microtopography of calcite is completely modified in the time it takes to scan the surface (~30 s). The crystallographic orientation of these new triangular etch pits as well as of the primary rhombic etch pits, are shown in Fig. 2*a,b*. As measured from the *in situ* AFM data, the increase of the etch pit area (A in mm^2) is rapid and is linearly correlated to the interaction time (t in s) in the early stages (up to 3 min) according to the relationship: $A = 19.7t - 6$. The dissolution is

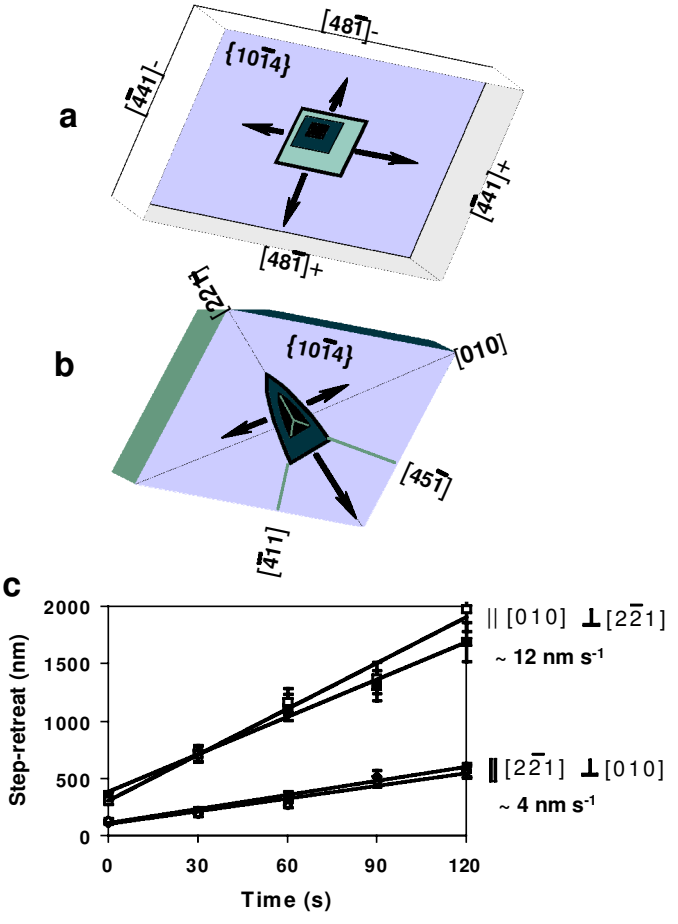

FIG. 2. Schematic diagrams indicating the replacement of a H_2O-induced rhombic etch pit (*a*) by a $Hg(CH_3COO)_2$-induced triangular etch pit, (*b*) as related to different crystallographic directions on the {10$\bar{1}$4} cleavage surface of calcite. The different step-retreat velocities of the new etch pit, are shown schematically by the length of the arrows in (*b*). The measurement of the velocities (*c*) is based on *in situ* AFM from the development of two well-defined etch pits.

strongly anisotropic with steps retreating faster along the [2$\bar{2}$1] direction than along the [010] direction (~12 nm s^{-1} and ~4 nm s^{-1}, respectively, as shown in Fig. 2*c*). The $Hg(CH_3COO)_2$-induced step-retreat velocity along [2$\bar{2}$1] is much greater than that recorded by Giudici (2002), for 'positive' steps of rhombic etch pits in the presence of HCl solution of lower initial pH (2.7). The height of the steps constituting the walls of the etch pits is ~3 Å (corresponding to one atomic layer of calcite). After ~5 min of interaction, the triangular etch pits begin to overlap eventually developing larger hexagonal-shaped etch pits (see text below).

Such a modification of the etch pit morphology has not been observed previously on calcite in the presence of foreign metal ions or other chemical constituents. Some morphological characteristics, such as the acute upper end, are similar to the etch pits described by Hong *et al.* (1997) for the interaction of calcite with maleic acid at pH <5. The formation of these elongated oval etch pits with pointed ends along [2$\bar{2}$1] was explained by the adsorption of the Mal^{2-} ion by pairs of Ca^{2+} ions into the initial rhombic etch pits. Elongated oval etch pits with edges along [010] have been described by Godelitsas *et al.* (2003) for the interaction of calcite with Pb^{2+} ions. Etch pits exhibiting a considerably different triangular morphology (equilateral without curved sides) and different crystallographic orientation, have been reported by Teng and Dove (1997) during the interaction of calcite with aspartate molecules. To test whether the CH_3COO^- ions might control the development of the triangular etch pits observed in the present study, separate *in situ* AFM experiments were carried out using only acetic acid and retaining the same pH conditions, although, necessarily, a different ionic strength (see the Experimental methods section, above). The results, shown in Fig. 3, indicated rhombic etch pits, similar to those observed in the presence of H_2O. There is, therefore, no indication that the presence of acetate, at least at concentration 0.006 M, can induce the formation of triangular etch pits, and it is the presence of Hg(II) ions that controls the new etch pit morphology.

'Positive' and 'negative' growth steps, analogous to dissolution steps formed on the {10$\bar{1}$4} surface of calcite during dissolution processes, also exist at polygonized hillocks which are developed onto the surface during growth processes in the presence of trace ions (impurities). The non-equivalence of growth steps is considered to be crucial for the preferential incorporation of foreign ions into the structure of calcite during crystal growth from a Ca^{2+}-NH_4^+-Cl^- growth solution (Paquette and Reeder, 1995). Certain cations (e.g. Sr^{2+}, Pb^{2+}) and anions (e.g. SO_4^{2-}, SeO_4^{2-}) which are larger than the potentially substituted structural ions ($^{[6]}Ca^{2+}$, CO_3^{2-}) tend to incorporate in 'large' sites located along 'positive' steps, whereas cations which are smaller than $^{[6]}Ca^{2+}$ (e.g. Mg^{2+}, Mn^{2+}, Co^{2+}, Cd^{2+}) tend to incorporate in 'small' sites located along 'negative' steps (Staudt *et al.*, 1994; Paquette and Reeder, 1995). Since there are no studies concerning growth features in the presence of Hg(II), it could be assumed that Hg^{2+} ions may similarly be incorporated in the surface structure of calcite during dissolution. In particular, they could react at relevant 'large' $[\bar{4}41]_+/[48\bar{1}]_+$ sites (intersections of obtuse dissolution steps) of pre-existing rhombic etch pits contributing to the stabilization of [010] (see also Fig. 2). However, the formation of the specific etch pit shape observed here cannot be easily explained by a simple preferential adsorption.

A comparison of the topography in Fig. 1*a* and *b* suggests that many layers of the original calcite surface are rapidly removed after the injection of the lower-pH Hg(II) solution. The absence of a vertical height reference point for the initial calcite surface makes the total amount of carbonate solid removed difficult to estimate but

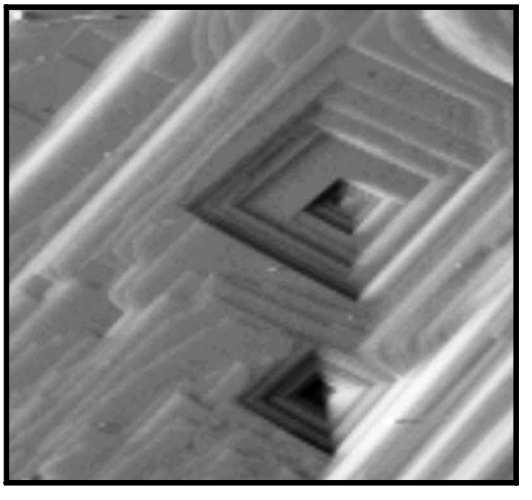

FIG. 3. *In situ* AFM image of the dissolved {10$\bar{1}$4} surface of calcite after injection of an CH_3COOH aqueous solution (pH $\approx$3.5). The scan area is 7.5×7.5 μm^2.

from the depth of the original H_2O-induced etch pits we estimate this to be at least 10 atomic layers (~30 Å). As a consequence, the novel triangular etch pits, described above, are immediately developed on the chemically modified surface. Furthermore, the dissolution of this modified surface proceeds intensely and anisotropically through the quick enlargement of the newly formed etch pits. The main characteristic of the modified {10$\bar{1}$4} surface relates to the existence of Hg(II), which is sorbed (adsorbed and perhaps also absorbed) at near-surface layers of the calcite structure and simultaneously regulates the evolution of the microtopography. On the other hand, there are also likely to be inhibiting effects on the dissolution which adjust the shape of the etch pits.

The XPS spectra of the calcite surface after 1 min and 5 min of interaction with $Hg(CH_3COO)_2$ aqueous solution are shown in Fig. 4 (depth of analysis ~30 Å). Quantification of the XPS spectra before and after interaction with the solution (taking into account peak areas and atomic sensitivity factors) indicates that though the initial Ca content (~40% w/w) of the near-surface layers is not significantly reduced after 1 min of interaction, the concentration of Hg(II) is detectable and reaches a value of 0.3%. The situation is clearer after 5 min of interaction; the surface concentration of Ca is considerably reduced (27.8%) while the related content of Hg(II) is increased (2.5%). The above data strongly suggest that Hg(II) ions are sorbed on calcite while its surface is dissolving. From the qualitative evaluation of the Ca $2p_{3/2}$ photoelectron peaks (e.g. Gopinath *et al.*, 2002), it is concluded that Ca^{2+} in the near-surface layers remains in a calcite-type structure during the interaction. Additionally, on the basis of the binding energy (BE) of the Hg $4f_{7/2}$ peaks resolved at 101.6 eV, the presence of elemental Hg (99.88 eV, Powell 1995) or the precipitation of HgO (100.77 eV, Humbert 1986) can be excluded. There are no XPS data on Hg(II) carbonate compounds in the literature and thus it is not possible to define the structural state of the sorbed Hg in the early stages of interaction. According to Hyland *et al.* (1990) who investigated the interaction of Hg(II) with pyrite and galena, as well as according to Ehrhardt *et al.* (2000) and Behra *et al.* (2001) who studied the interaction of Hg(II) with the pyrite surface, the

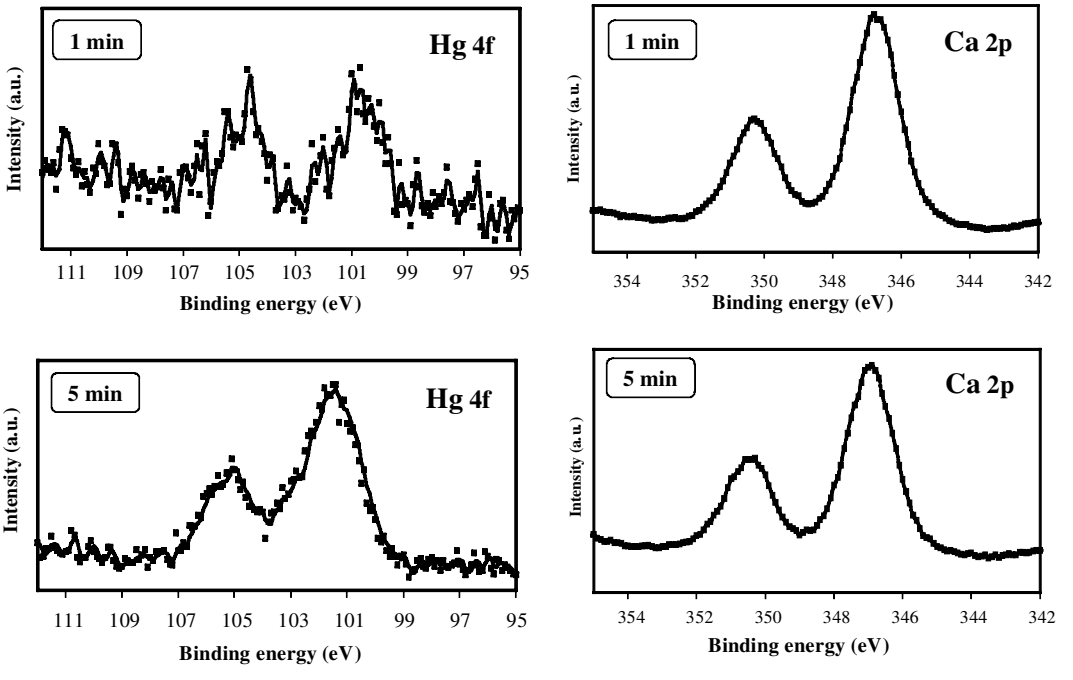

FIG. 4. XPS (Hg 4f and Ca 2p) data concerning the {10$\bar{1}$4} surface of calcite interacted for 1 min and 5 min with a Hg(II) solution. The spectra are correlated to the *in situ* AFM results presented in Fig. 1*b* and *d*.

Hg $4f_{7/2}$ BE of Hg(II) sorbed from solutions of low pH is in the region 100.7–100.9 eV due to surface complexes with sulphidic S. Consequently we may consider that the BE of Hg $4f_{7/2}$ recorded at higher energy in our experiments may be attributed to surface carbonate complexes of sorbed ions of Hg (II).

Furthermore, taking into account the extended literature on the interaction of other divalent metal ions with calcite, we could also argue the incorporation (absorption) of the metal in $^{[6]}Ca^{2+}$ surface sites. This allows us to speculate that a solid solution is formed on the surface of calcite, though with our existing data it is not possible to discuss the nature of such a material in the absence of information on a hypothetical $HgCO_3$ end-member. The incorporation of divalent metal ions into the calcite surface structure is generally discussed in terms of their size (e.g. Reeder, 1996). Common divalent metal ions (such as Mg^{2+}, Mn^{2+}, Fe^{2+}, Co^{2+}, Ni^{2+}, Cu^{2+}, Zn^{2+} and Cd^{2+}) occupy sixfold coordinated octahedral sites in the structure of carbonate solids, either as minor or major constituents. Under ambient conditions, they form pure carbonate phases with a trigonal calcite-type structure. However, Sr^{2+}, Ba^{2+} and Pb^{2+} may occur as minor constituents (impurities) in sixfold coordination (e.g. Reeder *et al.*, 1999) but possess a ninefold coordination as major constituents forming pure carbonates with an orthorhombic aragonite-type structure. In the first case, the ionic radii of all the divalent 6-coordinated metal ions, according to Shannon (1976), are smaller than that of $^{[6]}Ca^{2+}$, whereas in the second case the ionic radii of the divalent 6- and 9-coordinated metal ions are larger than those of $^{[6]}Ca^{2+}$ and $^{[9]}Ca^{2+}$ respectively ($^{[6]}r_{Ca^{2+}}$ = 1 Å and $^{[9]}r_{Ca^{2+}}$ = 1.18 Å). Taking into account that $^{[6]}r_{Hg^{2+}}$ = 1.02 Å (slightly larger than $^{[6]}r_{Ca^{2+}}$), it could be presumed that minor amounts of Hg^{2+} ions (impurities) can substitute Ca^{2+} ions in octahedral sites into the calcite structure. However, no $HgCO_3$ compound with either calcite or aragonite structure is known.

Longer term (5 min up to 1 month) interaction of calcite surface with Hg(II) solution

After longer-term interaction in the AFM fluid cell, the triangular etch pits observed during the first stages of the experiment are interconnected to form deep etch pits of hexagonal shape which are also developed along [2$\bar{1}$1] (Fig. 5). These etch pits continue to grow slowly till the end of the

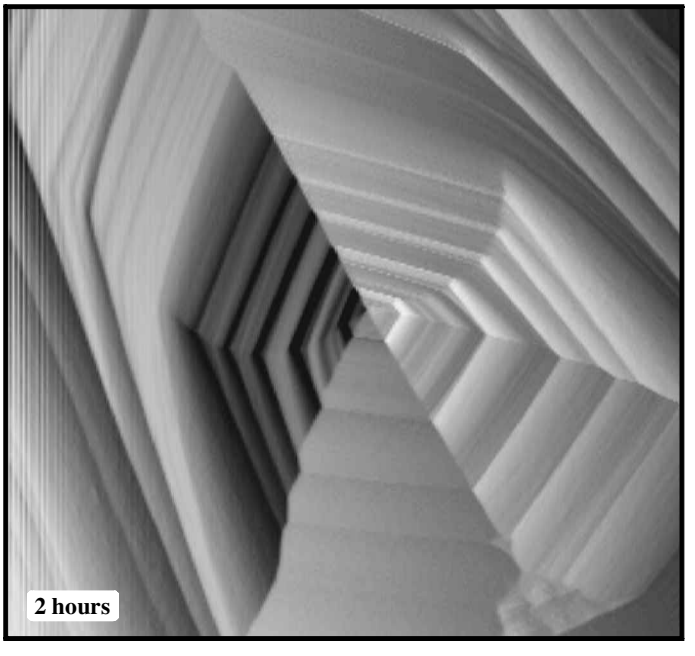

FIG. 5. *In situ* AFM image showing a hexagonal etch pit developed on the {10$\bar{1}$4} surface of calcite after ~2 h of interaction with $Hg(CH_3COO)_2$ aqueous solution. The scan area is 15×15 μm^2.

AFM study (~2 h) and remain stable, suggesting that the crystal almost reaches an equilibrium with the fluid in the cell. A later SEM-EDS investigation of the calcite crystal removed from the AFM fluid cell, showed the existence of extended dissolution features, on a micro-scale, too large to be observed by *in situ* AFM. Many of these large etch pits accommodate Hg-containing solid phases overgrown on the dissolved {10$\bar{1}$4} surface. As shown in Fig. 6, the aggregates of the Hg-containing flakes are perimetrically accompanied by small spheres which are supported on the calcite surface. Since the sorption phenomenon is apparently related to crystal growth of Hg(II) phases through a heterogeneous nucleation process, these spheres may be the earliest stages of the crystallization, although apart from the analytical evidence (by SEM-EDS) that they contain Hg, their nature is not known.

To determine the Hg(II) phases overgrown on the {10$\bar{1}$4} surface of calcite, separate *ex situ* experiments were also performed over longer periods of time. After 12 h of interaction, brown-red aggregates, macroscopically obvious, are developed on the calcite substrate. The SEM-EDS investigation showed that the aggregates consist of scattered tufts with well developed sphenoidal Hg-containing crystals (Fig. 7*a,b*). The powder-XRD investigation of some of these aggregates removed from the surface of calcite showed that the diffraction patterns of the Hg-containing crystals are consistent with synthetic orthorhombic HgO (Roth, 1956; Aurivillius, 1956) which is similar to the rare mineral montroydite (e.g. Woodhouse, 1934). Moreover, it was found that the patterns are almost identical to those corresponding to natural montroydite crystals, coexisting with elemental Hg, in speci-

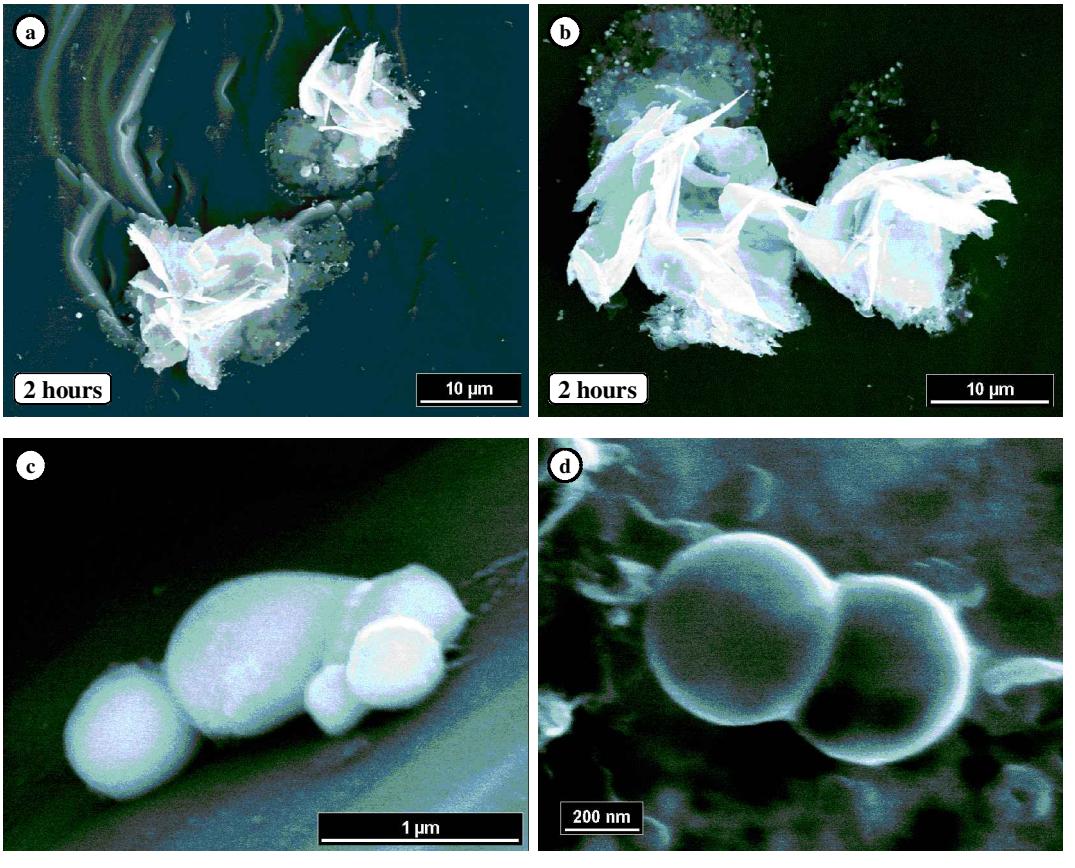

FIG. 6. SEM images of µm-sized Hg-containing flakes (*a,b*) grown onto the dissolved {10$\bar{1}$4} surface of the calcite crystal removed from the AFM fluid cell after ~2 h of interaction. The Hg-containing nm-sized spheres surrounding the flakes are also shown at higher magnification (*c,d*).

mens from Socrates mine, California, USA. In addition, FT-IR spectra indicated that the overgrown HgO is hydrated, giving the typical absorption bands of the H_2O molecule at 3445 cm^{-1} and 1634 cm^{-1}, as well as two peaks (at 584 cm^{-1} and 484 cm^{-1}), possibly due to Hg-O bonds. The SEM-EDS investigation of calcite samples exposed for 1 month to a $Hg(CH_3COO)_2$ solution, showed overgrown aggregates with more isometric crystals (Fig. 7*c,d*). Although there is an obvious change in the morphology of the crystals, the powder-XRD data indicate that they also correspond to a montroydite-type HgO. It should be noted that speciation calculations using the PHREEQC program (Parkhurst and Appelo, 1999) also show the formation of montroydite on the surface of calcite during either short or longer-term interaction with 5 mM Hg(II) in aqueous solution. It is particularly indicated that any increase of the initial pH value at ~3.5, due to the dissolution of the calcite surface, corresponds to a considerable increase of the supersaturation with respect to montroydite which appears to be a more stable phase in the system (Hg(II) hydroxide, which may formed, is unstable).

On the other hand, the expectation that, in common with other earlier studies concerning divalent metal ions, a Hg-bearing carbonate phase may form on the surface of calcite, has not been borne out in this work. According to Hietanen and Högfeldt (1976*a,b*), pure $HgCO_3$ solid has never been isolated in the Hg(II)-carbonate system, although several basic salts, such as $HgCO_3 \cdot 2HgO$, are known. The precipitation of these salts often results in the formation of HgO or compounds with very similar powder patterns to HgO, depending on the pH, despite the fact that

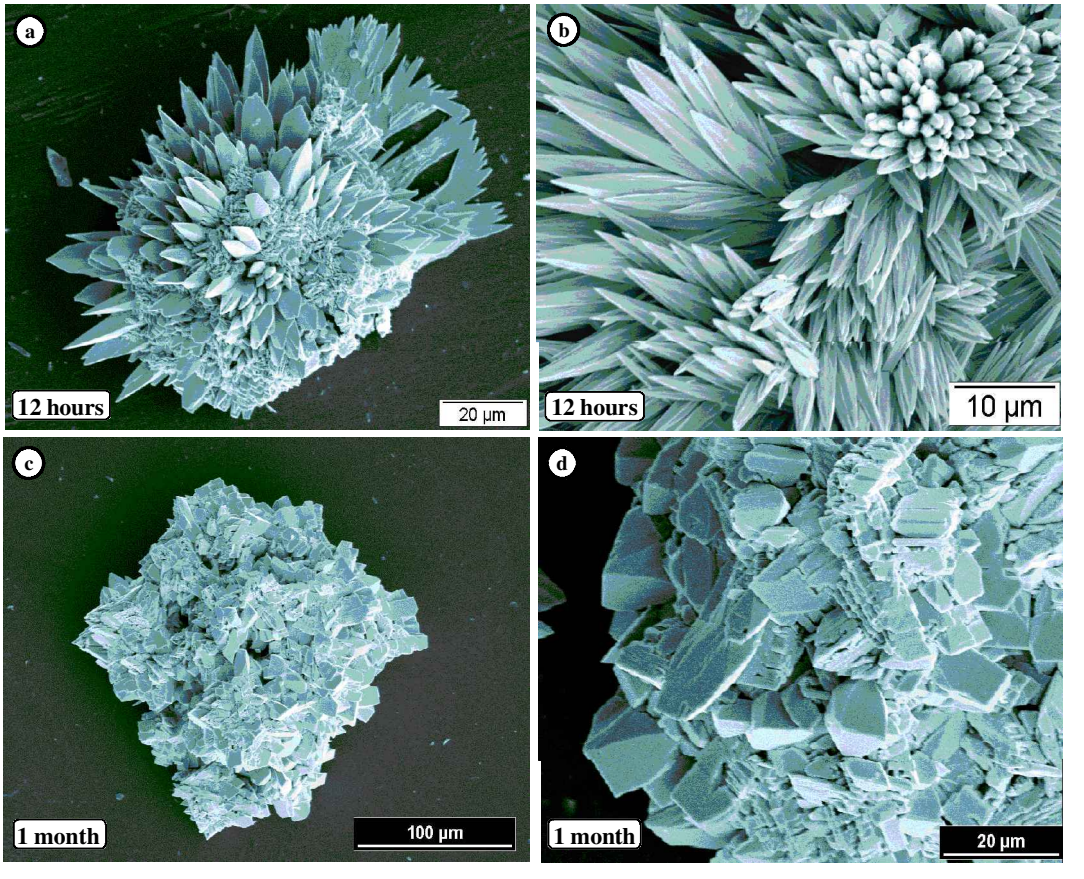

FIG. 7. SEM images of montroydite-type Hg(II) oxide crystal aggregates developed on calcite after ~12 h (*a,b*) and ~1 month of interaction (*c,d*) with a $Hg(CH_3COO)_2$ aqueous solution of 5 mM Hg(II).

complicated synthesis methods have also been suggested (Jordan *et al.*, 1966; Bilinski *et al.*, 1980). The crystal structure of the Hg(II) basic carbonates remains unknown. The powder-XRD card of $HgCO_3{\cdot}2HgO$ (#32-0657, ® 2000 JCPDS), based on the data of Bilinski *et al.* (1980), does not contain information on the crystal system and the unit-cell constants. Thus the thermodynamic properties of a hypothetical solid solution $(Ca,Hg)CO_3$ or $(Hg,Ca)CO_3{\cdot}2HgO$ are completely unknown. Furthermore, according to Khodakovskiy and Shikina (1981), $HgCO_3{\cdot}HgO$ is unstable under Earth's atmospheric conditions and should spontaneously lose CO_2 to produce montroydite (which is stable even at very high CO_2 pressures) according to the reaction: $HgCO_3{\cdot}HgO \rightarrow 3HgO + CO_{2\,(g)}$.

Conclusions

In situ AFM experiments showed that typical H_2O-induced rhombic etch pits formed on the $\{10\bar{1}4\}$ cleavage surface of calcite, are rapidly transformed to deeper etch pits exhibiting an unusual triangular shape, after interaction with $Hg(CH_3COO)_2$ aqueous solution of 5 mM Hg(II) and pH ≈3.5, at room temperature under atmospheric P_{CO_2}. The new $Hg(CH_3COO)_2$-induced etch pits move faster along the $[2\bar{2}1]$ direction than along the [010] direction (with step-retreat velocities of ~12 nm s^{-1} and ~4 nm s^{-1}, respectively), indicating an anisotropic dissolution process. Relevant microscopic data, concerning the interaction of calcite with CH_3COOH, indicated a minor influence of the corresponding anions, and that the contribution of Hg(II) cations is more crucial with respect to sorption processes and inhibiting effects during the surface dissolution. The sorption of Hg(II) (adsorption and probably absorption also) in the dissolved surface during the first minutes of the interaction, most probably at $^{[6]}Ca^{2+}$ sites, is supported by spectroscopic (XPS) data. Furthermore, the triangular etch pits are interconnected to form larger hexagonal etch pits, while Hg(II) phases (obvious by SEM) have already grown on the surface through a heterogeneous nucleation process. The crystal growth of orthorhombic (montroydite-type) hydrated Hg(II) oxide ($HgO{\cdot}nH_2O$) on the surface of calcite, as a result of the metal removal, was proved at samples exposed for longer times to $Hg(CH_3COO)_2$ solution. The formation of potential Hg(II) carbonates ($HgCO_3$ and/or $HgCO_3{\cdot}2HgO$), as might be expected on the basis of previous studies on the interaction of divalent metal ions and calcite, was not confirmed in the present study.

Acknowledgements

We would like to thank the European Commission for support within the frameworks of the European Research Training Network on 'Quantifying Dissolution and Precipitation of Solid-Solutions in Natural and Industrial Processes' (contract HPRN-CT-2000-00058) and the Marie Curie Fellowships Programme. We also acknowledge the support of the European Community Access to Research Infrastructure action of the Improving Human Potential Programme (contract HPRI-CT-1999-00008 awarded to Prof. B.J. Wood, EU Geochemical Facility, University of Bristol, UK). Many thanks are finally due to U. Breit (Inst. Mineralogie, Univ. Münster) for collaboration during the SEM-EDS investigations.

References

Astilleros, J.M., Pina, C.M., Fernández-Díaz, L. and Putnis, A. (2000) The effect of barium on calcite $\{10\bar{1}4\}$ surfaces during growth. *Geochimica et Cosmochimica Acta*, **64**, 2965–2972.

Astilleros, J.M., Pina, C.M., Fernández-Díaz, L. and Putnis, A. (2002) Molecular-scale surface processes during the growth of calcite in the presence of manganese. *Geochimica et Cosmochimica Acta*, **66**, 3177–3189.

Astilleros, J.M., Pina, C.M., Fernández-Díaz, L. and Putnis, A. (2003) Metastable phenomena on calcite $\{10\bar{1}4\}$ surfaces growing from Sr^{2+}-Ca^{2+}-CO_3^{2-} aqueous solutions. *Chemical Geology*, **193**, 93–107.

Aurivillius, K. (1956) The crystal structure of mercury(II) oxide studied by X-ray and neutron diffraction methods. *Acta Chemica Scandinavica*, **10**, 852–866.

Baes, C.F. and Mesmer, R.E. (1986) *The Hydrolysis of Cations*. Krieger Publishing Co., Malabar, Lord Howe Island, Australia.

Behra, P., Bonnissel-Gissinger, P., Alnot, M., Revel, R. and Ehrhardt, J.-J. (2001) XPS and XAS study of the sorption of Hg(II) onto pyrite. *Langmuir*, **17**, 3970–3979.

Bilinski, H., Marković, M. and Gessner, M. (1980) Solubility and equilibrium constants of mercury(II) in carbonate solutions (25 ºC, I=0.5 mol dm^{-3}). *Inorganic Chemistry*, **19**, 3440–3443.

Britt, D.W. and Hlady, V. (1997) *In situ* atomic force

microscope imaging of calcite etch pit morphology changes in undersaturated and 1-hydroxyethylidene-1,1-diphosphonic acid poisoned solutions. *Langmuir*, **13**, 1873–1876.

Davis, K.J., Dove, P.M. and De Yoreo J.J. (2000) The role of Mg^{2+} as an impurity in calcite growth. *Science*, **290**, 1134–1137.

De Giudici, G. (2002) Surface control vs. diffusion control during calcite dissolution: Dependence of step-edge velocity upon solution pH. *American Mineralogist*, **87**, 1279–1285.

Ehrhardt, J.J., Behra, P., Bonnissel-Gissinger, P. and Alnot, M. (2000) XPS study of the sorption of Hg(II) onto pyrite FeS_2. *Surface and Interface Analysis*, **30**, 269–272.

Godelitsas, A., Astilleros, J.M., Hallam, K., Harissopoulos, S. and Putnis, A. (2003) Interaction of calcium carbonates with lead in aqueous solutions. *Environmental Science & Technology*, **37**, 3351–3360

Gopinath, C.S., Hegde, S.G., Ramaswamy, A.V. and Mahapatra, S. (2002) Photoemission studies of polymorphic $CaCO_3$ materials. *Materials Research Bulletin*, **37**, 1323–1332.

Hay, M.B., Workman, R.K. and Manne, S. (2003) Mechanisms of metal ion sorption on calcite: Composition mapping by lateral force microscopy. *Langmuir*, **19**, 3727–3740.

Hietanen, S. and Högfeldt, E. (1976*a*) A potentiometric study of the solid phases in the systems Hg(I)-HCO_3^- and Hg(II)-HCO_3^-. *Chemica Scripta*, **9**, 24–29.

Hietanen, S. and Högfeldt, E. (1976*b*) On the complex formation between Hg(II) and CO_3^{2-}. *Chemica Scripta*, **10**, 37–38.

Hillner, P.E., Gratz, A.J., Manne, S. and Hansma, P.K. (1992) Atomic-scale imaging of calcite growth and dissolution in real time. *Geology*, **20**, 359–362.

Hoffman, U. and Stipp, S.L.S. (2001) The behavior of Ni^{2+} on calcite surfaces. *Geochimica et Cosmochimica Acta*, **65**, 4131–4139.

Hong, Q., Suárez, M.F., Coles, B.A. and Compton, R.G. (1997) Mechanism of solid/liquid interfacial reactions. The maleic acid driven dissolution of calcite: An atomic force microscopy study under defined hydrodynamic conditions. *Journal of Physical Chemistry B*, **101**, 5557–5564.

Humbert, P. (1986) An XPS and UPS photoemission study of HgO. *Solid State Communications*, **60**, 21–24.

Hyland, M.M., Jean, G.E. and Bancroft, G.M. (1990) XPS and AES studies of Hg(II) sorption and desorption reactions on sulphide minerals. *Geochimica et Cosmochimica Acta*, **54**, 1957–1967.

Jordan, R.B., Sargeson, A.M. and Taube, H. (1966) The mechanism of the reaction of carbonato-pentaamminecobalt(II) with divalent ions. *Inorganic Chemistry*, **5**, 486–488.

Kamiya, N., Kagi, H., Notsu, K., Tsuno, H. and Akagi, T. (2002) Inhibiting effects of trace amounts of lanthanum ion on the dissolution of calcite: A comparative study on calcium carbonate polymorphs. *Chemical Letters*, 890–891.

Khodakovskiy, I.L. and Shikina, N.D. (1981) The role of carbonate complexes in mercury transport in hydrothermal solutions (experimental studies and thermodynamic analysis). *Geokhimiya*, **5**, 671–682.

Lea, A.S., Amonette, J.E., Baer, D.R., Liang, Y. and Colton, N.G. (2001) Microscopic effects of carbonate, manganese, and strontium ions on calcite dissolution. *Geochimica et Cosmochimica Acta*, **65**, 369–379.

Lea, A.S., Hurt, T.T., El-Azab, A., Amonette, J.E. and Baer, D.R. (2003) Heteroepitaxial growth of a manganese carbonate secondary nano-phase on the (1014) surface of calcite in solution. *Surface Science*, **524**, 63–77.

Liang, Y. and Baer, D.R. (1997) Anisotropic dissolution at the $CaCO_3$ (10$\bar{1}$4)-water interface. *Surface Science*, **373**, 275–287.

Liang, Y., Baer, D.R., McCoy, J.M. and LaFemina, J.P. (1996) Interplay between step velocity and morphology during the dissolution of $CaCO_3$ surface. *Journal of Vacuum Science and Technology*, **A14**, 1368–1375.

Orme, C.A., Noy, A., Wierzbicki, A., McBride, M.T., Grantham, M., Teng, H.H., Dove, P.M. and De Yoreo, J.J. (2001) Formation of chiral morphologies through selective binding of amino acids to calcite surface steps. *Nature*, **411**, 775–779.

Paquette, J. and Reeder, R.J. (1995) Relationship between surface structure, growth mechanism, and trace element incorporation in calcite. *Geochimica et Cosmochimica Acta*, **59**, 735–749.

Parkhurst, D.L. and Appelo, C.A.J. (1999) *User's guide to PHREEQC (Version 2) – A computer program for speciation, batch-reaction, one-dimensional transport, and inverse geochemical calculations*. US Geological Survey Water-Resources Investigations Report **99-4259**, 312 pp.

Powell, C.J. (1995) Elemental binding energies for X-ray photoelectron spectroscopy. *Applied Surface Science*, **89**, 141–149.

Putnis, A., Pina, C.M., Astilleros, J.M., Fernandez-Diaz, L. and Prieto, M. (2003) Nucleation of solid solutions crystallizing from aqueous solutions. *Philosophical Transactions of the Royal Society of London*, **A361**, 1–17.

Reeder , R.J. (1996) Interaction of divalent cobalt, zinc, cadmium, and barium with the calcite surface during layer growth. *Geochimica et Cosmochimica Acta*, **60**, 1543–1552.

Reeder, J.R., Lamble, G.M. and Northrup, P.A. (1999) XAFS study of the coordination and local relaxation around Co^{2+}, Zn^{2+}, Pb^{2+}, and Ba^{2+} trace elements in calcite. *American Mineralogist*, **84**, 1049–1060.

Rimstidt, J.D., Balog, A. and Webb, J. (1998) Distribution of trace elements between carbonate minerals aqueous solutions. *Geochimica et Cosmochimica Acta*, **62**, 1851–1863.

Roth, W.L. (1956) The structure of mercuric oxide. *Acta Crystallographica*, **9**, 277–280.

Shannon, R.D. (1976) Revised effective ionic radii and systematic studies of interatomic distances in halides and chalcogenides. *Acta Crystallographica*, **A32**, 751–767.

Shiraki, R., Rock, P.A. and Casey, W.H. (2000) Disolution kinetics of calcite in 0.1 M NaCl solution at room temperature: An Atomic Force Microscopic (AFM) study. *Aquatic Geochemistry*, **6**, 87–108.

Staudt, W.J., Reeder, R.J. and Schoonen, M.A.A. (1994) Surface structural controls on compositional zoning of SO_4^{2-} and SeO_4^{2-} in synthetic calcite crystals. *Geochimica et Cosmochimica Acta*, **58**, 2087–2098.

Stipp, S.L.S., Hochella Jr., M.F., Parks, G.A. and Leckie, J.O. (1992) Cd^{2+} uptake by calcite, solid-state diffusion, and the formation of solid solutions: Interface processes observed with near-surface sensitive techniques (XPS, LEED, and AES). *Geochimica et Cosmochimica Acta*, **56**, 1941–1954.

Stipp, S.L.S., Eggleston, C.M. and Nielsen, B.S. (1994) Calcite surface structure observed at microtopographic and molecular scales with atomic force microscopy (AFM). *Geochimica et Cosmochimica Acta*, **58**, 3023–3033.

Stipp, S.L.S., Lakshtanov, L.Z., Jensen, J.T. and Baker, J.A. (2003) Eu^{3+} uptake by calcite: Preliminary results from coprecipitation experiments and observations with surface-sensitive techniques. *Journal of Contaminant Hydrology*, **61**, 33–43.

Temmam, M., Paquette, J. and Vali, H. (2000) Mn and Zn incorporation into calcite as a function of chloride aqueous concentration. *Geochimica et Cosmochimica Acta*, **64**, 2417–2430.

Teng, H.H. and Dove, P.M. (1997) Surface site-specific interactions of aspartate with calcite during dissolution: Implications for biomineralization. *American Mineralogist*, **82**, 878–887.

Teng, H.H., Dove, P.M., Orme, C.A. and De Yoreo, J.J. (1998) Thermodynamics of calcite growth: Baseline for understanding biomineral formation. *Science*, **282**, 724–727.

Tesoriero, A.J. and Pankow, J.F. (1996) Solid solution partitioning of Sr^{2+}, Ba^{2+}, and Cd^{2+} to calcite. *Geochimica et Cosmochimica Acta*, **60**, 1053–1063.

Woodhouse, C.D. (1934) A new occurrence of montroydite in California. *American Mineralogist*, **19**, 603–604.

[*Manuscript received 31 January 2003: revised 24 July 2003*]